Geol. Mag. **146** (5), 2009, pp. 732–742. © 2009 Cambridge University Press
doi:10.1017/S0016756809006438 *Printed in the United Kingdom*

Late Miocene magmatic activity in the Attic-Cycladic Belt of the Aegean (Lavrion, SE Attica, Greece): implications for the geodynamic evolution and timing of ore deposition

ANTHI LIATI*†, NIKOS SKARPELIS‡ & GEORGIA PE-PIPER§

*Institute of Isotope Geology and Mineral Resources, ETH Zurich, Clausiusstrasse 25, 8092 Zurich, Switzerland
‡Department of Geology & Geoenvironment, University of Athens, Panepistimiopoli, 15784 Zografou, Athens, Greece
§Department of Geology, Saint Mary's University, Halifax, NS B3H 3C3, Canada

(*Received* 21 May 2008; *accepted* 20 November 2008; First published online 15 July 2009)

Abstract – Numerous post-metamorphic Miocene granitoids occur in the area of Lavrion, SE Attica, at the western end of the Attic-Cycladic Belt of the Aegean. U–Pb ion microprobe-dating (SHRIMP) of zircon from a granitoid sill in the hanging-wall of a regional detachment fault reveals two distinct ages: (1) 11.93 ± 0.41 Ma, obtained from inherited zircon cores with metamorphic characteristics (homogeneous cathodoluminescence, low Th/U ratios) and granulite-type (round/resorbed) morphology. This age is interpreted as the time of a likely granulite-facies metamorphism of the precursor rock. (2) 8.34 ± 0.20 Ma, obtained by oscillatory zoned zircon domains with cathodoluminescence and Th/U characteristics typical for magmatic origin. This age is interpreted as the crystallization time of the granitoid sills. Although a granulite-facies metamorphic event has not been recognized so far for rocks of the Attic-Cycladic Belt, it seems to be the most plausible hypothesis to explain both the zircon systematics and age results. This hypothesis is consistent with an extensional regime predominating in the Aegean from Late Miocene times onwards. A possible granulite-facies metamorphism can be related to magmatic underplating at the initial stages of extension, setting an upper age of *c.* 12 Ma for the operation of the detachment fault. The 8.34 ± 0.20 Ma zircon crystallization age is, statistically, marginally different to a previous K–Ar feldspar date of hornblende-bearing dykes (9.4 ± 0.3 Ma) and identical to a 8.27 ± 0.11 Ma K–Ar biotite date of the main granitoid stock in the area, thus being generally consistent with prior age constraints from the region. Operation of the detachment fault in the Lavrion area is therefore bracketed between *c.* 11.9 Ma and at least 8.3 Ma. This time range is in line with the time of operation of detachment faults suggested previously for the Cycladic islands. Carbonate-hosted replacement-type massive sulphide Pb–Zn–Ag ores are spatially associated with the detachment fault and related extensional structures in the Basal Unit. Therefore, these Pb–Zn–Ag ores probably also formed within the above time span of *c.* 11.9 to at least 8.3 Ma. U–Pb ion microprobe (SHRIMP) dating of zircon from an orthogneiss within the metaclastic subunit of the Basal Unit in Lavrion yielded a protolith age of 240 ± 4 Ma, consistent with ages of Triassic volcanism elsewhere in Greece.

Keywords: SHRIMP-dating, granitoid sills, sulphide ore, Attic-Cycladic Belt, Lavrion granulite-facies.

1. Introduction

The mid- to late Miocene magmatic activity in the Attic-Cycladic Belt of the Aegean (Fig. 1) is closely related to extensional tectonics in an arc setting. This magmatic activity was followed by the formation of the South Aegean Active Volcanic Arc in the Pliocene, connected to the subduction of the African plate underneath the Aegean microplate that continues today. The Cycladic islands, together with Attica (Fig. 1), are currently in a back-arc position. The Aegean Sea has extended by about 250 km since Early Miocene times (e.g. McKenzie, 1978). Extension was accommodated by low-angle normal (detachment) faults (Lister, Banga & Feenstra, 1984; Avigad *et al.* 1997). Miocene igneous activity was to a great extent controlled by local extensional structures, related to this large-scale extension in the Aegean (Faure, Bonneau & Pons, 1991; Pe-Piper & Piper, 2002). Granitoid plutons in the Cyclades were emplaced syn-tectonically to major detachment faults between *c.* 15 and 9 Ma (Altherr *et al.* 1982; Keay, Lister & Buick, 2001; Altherr & Siebel, 2002; Brichau *et al.* 2006 and references therein).

Miocene extensional tectonics and magmatism are well understood in the Cycladic islands but the western end of the Attic-Cycladic belt in Lavrion, SE Attica, has been inadequately studied. The area of Lavrion (Fig. 1) includes Miocene igneous rocks and both skarn-type and widespread carbonate-hosted replacement-type massive sulphide–Pb–Zn–Ag mineralization (Marinos & Petrascheck, 1956). The dominant magmatic rock-type is a late Miocene granodiorite stock at Plaka (Fig. 2). Granitoid dykes occur at the footwall of a detachment fault separating the two principal tectonic units in the area (see Section 2.b). Hydrothermally

*Author for correspondence: anthi.liati@empa.ch
†Present address: EMPA, Swiss Federal Laboratories for Materials Testing and Research, Ueberlandstrasse 129, CH-8600, Dübendorf, Switzerland

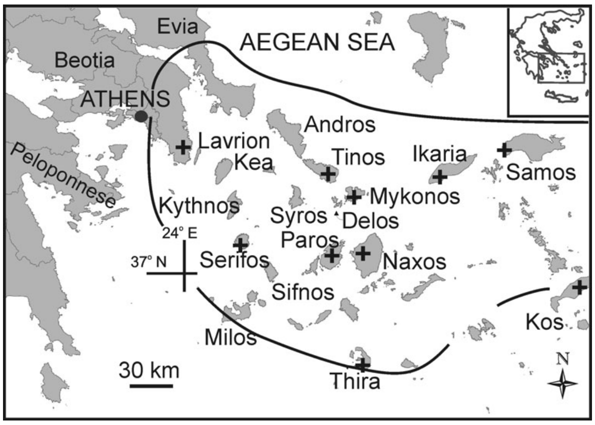

Figure 1. Map of the southern Aegean region indicating the extent of the Attic-Cycladic Belt and locations as discussed in the text. Major Miocene granitoids are marked by a cross.

altered porphyritic granitoids in the form of sills are associated with the detachment fault (Skarpelis, 2007). Because of their mode of occurrence and their spatial relationship to the detachment (see details in Section 3.a), these sills are considered as key rock-types for having the potential to provide information and put constraints on: (1) the timing of movement on the detachment fault, (2) how this time compares with that suggested for extensional faulting and related magmatic activity in other parts of the Attic-Cycladic Belt, and (3) the time of deposition of the ore mineralization, since the detachment and related structures in the footwall acted as conduits for mineralizing fluids.

Within the framework of the present study, a granitoid sill in the hanging-wall of the detachment fault was chosen for radiometric dating, as the most suitable rock-type to clarify the three issues addressed above. Further implications of the radiometric dating are connected with the geodynamic framework during the time of formation of this rock-type, in conjunction with the time of igneous activity in the Attic-Cycladic Belt, which coincides with the time of extensional tectonics (see Section 2.a). It is worth mentioning that rocks with a similar mode of occurrence have not yet been found elsewhere in the Attic-Cycladic Belt. Moreover, in order to clarify the time of igneous activity in the lower unit (the 'Basal Unit'; see Section 2.b) prior to metamorphism and understand better its geotectonic position, an orthogneiss was also included for dating in the present study.

Due to the complex formation history of the rocks and their strong interaction with fluids, which usually results in disturbances of commonly used isotopic systems such as the K–Ar or the Rb–Sr system, U–Pb ion microprobe dating (SHRIMP) of zircon, assisted by cathodoluminescence (CL) imaging, was applied as the most suitable technique. Furthermore, the SHRIMP-dating technique has the advantage of potentially dating multiple zircon generations within a single crystal. Thus, for the granitoid included in this study, this method has the potential of dating parts of zircon eventually inherited from the source rock from which the magma was produced (compare, for example, Vavra, Schmid & Gebauer, 1999).

2. Geological setting

2.a. Geology of the Attic-Cycladic Belt

The Lavrion area in SE Attica forms the western end of the Attic-Cycladic Belt (Fig. 1). The principal tectonic units in the Attic-Cycladic Belt are the 'Cycladic Blueschist Unit' and the 'Basal Unit'. The 'Cycladic Blueschist Unit' comprises mainly pre-Alpine basement orthogneisses and metamorphosed Permian–Mesozoic carbonate and clastic sedimentary rocks, mafic and felsic volcanic rocks and serpentinites (e.g. Dürr *et al.* 1978; Henjes-Kunst & Kreuzer, 1982; Andriessen, Banga & Hebeda, 1987; Okrusch & Bröcker, 1990). This unit underwent high pressure (HP), blueschist- to eclogite-facies metamorphism during Eocene times ($\sim$ 12–20 kbar, $\sim$ 450–550 °C: e.g. Altherr *et al.* 1979, 1982; Matthews & Schliestedt, 1984; Wijbrans & McDougall, 1988; Bröcker *et al.* 1993; Tomaschek *et al.* 2003) and a medium-pressure, Barrovian overprint at the Oligocene/Miocene boundary ($\sim$ 5–9 kbar, $\sim$ 450–550 °C: e.g. Bröcker *et al.* 1993). In the southern Cyclades, the overprint culminated in anatectic processes and the formation of thermal domes (e.g. Jansen & Schuiling, 1976; Altherr *et al.* 1979, 1982; Wijbrans & McDougall, 1988). In Attica, Evia island and a few Cycladic islands, the Cycladic Blueschist Unit is structurally underlain by the Basal Unit, considered to be part of the External Hellenides (Godfriaux, 1968; Katsikatsos *et al.* 1986). The Basal Unit comprises Mesozoic platform carbonates and a Tertiary anchimetamorphic flysch (e.g. Dürr *et al.* 1978; Dubois & Bignot, 1979; Bonneau, 1984). High-pressure metamorphism in the Basal Unit ($\sim$ 10 kbar, $\sim$ 350 °C) is dated at *c.* 23 Ma (Shaked, Avigad & Garfunkel, 2000; Ring, Layer & Reischmann, 2001; Ring & Reischmann, 2002).

Detachment faults in the Aegean islands and SE Attica were operating during Miocene times (e.g. Brichau *et al.* 2006). The detachment faults and associated wrench faults in the footwall and extensional listric faults in the hanging-wall led to crustal weakening and facilitated granite ascent (Pe-Piper, Piper & Matarangas, 2002) and fluid circulation (Skarpelis & Gilg, 2006; Skarpelis, 2007). Thus, granites were interpreted to have intruded syn-kinematically into the footwall of Miocene detachment faults (e.g. Faure, Bonneau & Pons, 1991; Lee & Lister, 1992). Alternatively, as suggested by Boronkay & Doutsos (1994), granitic magmas rose up along crustal-scale transpressive structures in some parts of the Aegean (e.g. Tinos, Serifos), whereas extension facilitated ascent and emplacement of granitoids in other parts (e.g. Mykonos, Paros, Naxos). The compositional variation of the plutonic rocks from east to west is remarkable: monzonite intrusions occur in the eastern part of the South Aegean (Kos, Samos), granite and granodiorite in the central Cyclades, and granodiorite in the western part (Serifos)

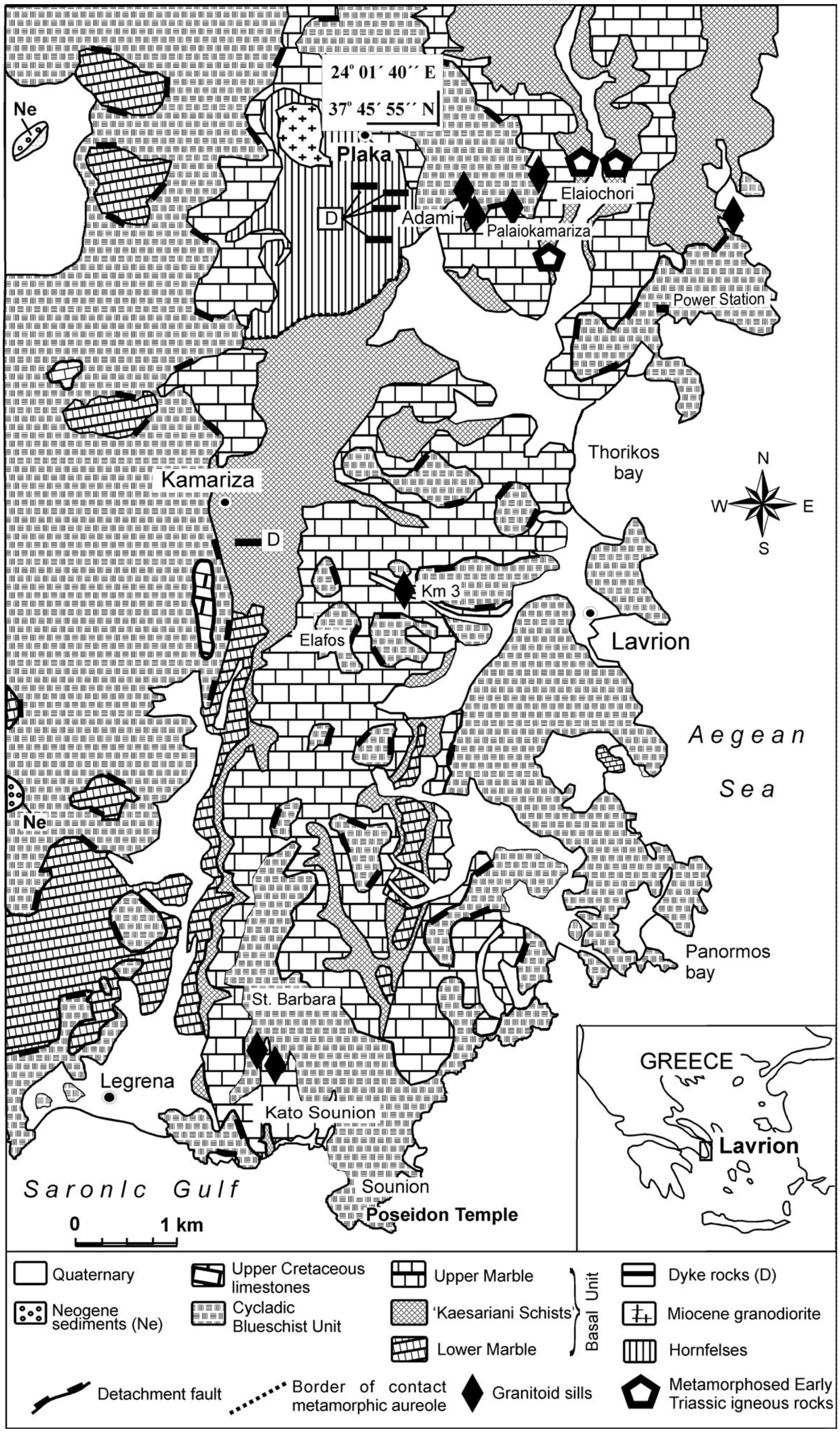

Figure 2. Geological map of Lavrion area (from Skarpelis, 2007) including outcrops of granitoid sills and the Early Triassic orthogneiss.

and in SE Attica (Fig. 1). Intrusions occur mostly as plutons and stocks, whereas dykes cross-cutting either metamorphic country rocks (Lavrion, Tinos, Andros) or granitoids (Delos, Serifos) are minor. I-type plutons predominate, whereas granites with S-type characteristics form small stocks or dykes (Naxos, Paros, Tinos, Ikaria: Altherr *et al.* 1982; Pe-Piper, Kotopouli & Piper, 1997; Pe-Piper, 2000; Pe-Piper, Piper & Matarangas, 2002). Minor arc-related volcanic rocks in the area range in age from *c.* 5 to 12 Ma (Fytikas *et al.* 1984).

2.b. Local geology: the Lavrion area

In SE Attica, a detachment fault juxtaposes the Basal Unit against rocks of the Cycladic Blueschist

https://doi.org/10.1017/S0016756809006438 Published online by Cambridge University Press

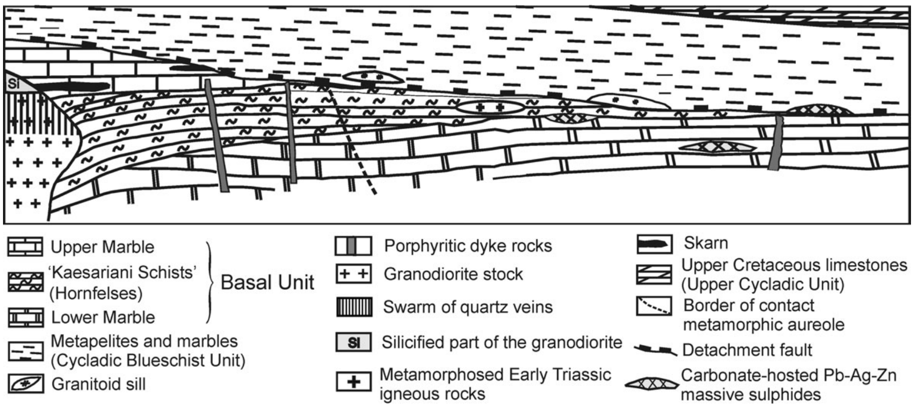

Figure 3. Schematic illustration showing the setting of the various igneous rocks at Lavrion area (not to scale). Modified from Skarpelis, Tsikouras & Pe-Piper (2008).

Unit (Figs 2, 3; Skarpelis, 2007). The Blueschist Unit comprises metapelites, metasandstones, marbles, metabasic rocks and minor quartzites. Metabasites experienced eclogite-facies through epidote/blueschist- to greenschist-facies metamorphism (Baltatzis, 1996). Based on a modified empirical Raman spectroscopy thermometer on carbonaceous material from mica-schists, peak metamorphic temperatures were estimated as around 320 °C (Baziotis, Mposkos & Skarpelis, 2006). The Basal Unit comprises HP/LT metaclastic rocks and intercalated orthogneisses (constituting a subunit known as 'Kaesariani schists': Marinos & Petrascheck, 1956) sandwiched between marbles. The early stages of the exhumation path of the metaclastic subunit are characterized by decompressional heating from 9–11 kbar at 320–350 °C to 5–6 kbar at ∼ 450 °C (Baziotis, Mposkos & Perdikatsis, 2006). Undeformed, sub-vertical dykes of porphyritic quartz-syenite to granodiorite and granite composition, as well as a slightly deformed and variably hydrothermally altered late Miocene granodiorite stock, intrudes the metamorphic rocks of the Basal Unit at the footwall of the detachment (Fig. 3).

A 9.4 ± 0.3 Ma K–Ar feldspar age from hornblende-bearing dykes below the detachment fault (Skarpelis, Tsikouras & Pe-Piper, 2008) provides a minimum time for the post-metamorphic igneous activity in the Basal Unit. A younger K–Ar biotite age of 8.27 ± 0.11 Ma and a *c.* 7.3 Ma apatite fission track age (Altherr *et al.* 1982) are reported for the Plaka granodiorite stock (Fig. 2). The E–W orientation of the porphyry dykes is indicative of a regional extensional stress field with roughly N–S direction (Skarpelis, Tsikouras & Pe-Piper, 2008).

Ore formation at Lavrion occurred under extensional kinematic conditions related to the formation of metamorphic core complexes in the Attic-Cycladic Belt. Skarn-type magnetite and base metal sulphide mineralization, as well as skarn-free replacements with Pb–Ag–Zn massive sulphide and pyrrhotite ore, occur within marbles in the contact metamorphic aureole of the Plaka granodiorite (Skarpelis, 2007). Non-skarn, carbonate-hosted replacement-type Pb–Ag–Zn massive sulphide ores are both structurally and lithologically controlled. The latter ore-types are partly conformable and/or partly cross-cutting the mylonitic foliation plane of marbles of the Basal Unit, along shear bands of the marbles or along the regional detachment fault (Fig. 3). Their mode of occurrence indicates that ore deposition by hydrothermal fluids took place mainly during the transitional ductile/brittle and brittle deformation stage of the host rocks (Skarpelis, 2007). The timing of ore deposition of non-skarn ores along those extensional structures can be indirectly inferred by dating granitoid sills associated with the detachment fault.

Late Cretaceous limestones (Leleu & Neumann, 1969) and thin slivers of ophiolitic ultramafic rocks tectonically overlie the Blueschist Unit and are possibly equivalent to rocks of the Upper Cycladic Unit cropping out in Paros and Naxos. Middle Miocene sediments, tectonically overlying the Blueschist Unit, comprise lacustrine and brackish-water deposits (Marinos & Petrascheck, 1956).

3. Description of the dated samples

The mode of occurrence and the petrological features of the dated rocks are briefly described here, in order to provide a basis for the interpretation of the geochronological data.

3.a. Granitoid sill

3.a.1. Mode of occurrence

The geological setting of the granitoid sills and their regional distribution are shown in Figures 2 and 3. The granitoid sills investigated are characterized by the absence of penetrative deformation, implying a late kinematic character for the intrusion with respect to the regional deformation of the Blueschist Unit. Contact metamorphism of the surrounding metamorphic rocks is not recognized, possibly due to the small volume of these igneous sills. Fast exhumation caused by rapid movement of the detachment fault may also have contributed to fast cooling of the sills and therefore lack of contact metamorphic phenomena in the immediately surrounding rocks. Minor hydrothermal alteration of country rock metapelites is observed close to contact with the sills, marked by the occurrence of chlorite, sericite, carbonates and opaque minerals (Fe and Mn hydroxides, and minor base metal sulphides) along thin fractures cross-cutting the foliation plane.

The sample of the granitoid sill dated in this study was collected from a 350 m long sill at Palaiokamariza village (Figs 2, 3; St Paul monastery, coordinates: N 37°45′35″, E 24°02′3″). It occurs in the hanging-wall of the detachment fault within a sequence of metapelites and marbles belonging to the Cycladic Blueschist Unit.

3.a.2. *Mineralogy, petrology*

The granitoid sill displays porphyritic texture, with coarse phenocrysts of white mica, exceeding 0.6 mm in length. The common mineral assemblage includes white mica, K-feldspar, quartz, zircon, monazite, Ti-oxide and discrete crystals of apatite. Based on its normative mineralogy, this rock type is classified as granite to granodiorite.

The rock is affected by strong hydrothermal alteration, as indicated by the presence of abundant sericite, carbonates (mainly Mg-calcite and dolomite), quartz, minor chlorite, anatase, sulphides (pyrite, galena) and high LOI (loss on ignition), ranging between 3 and 8.5 wt %. Fine-grained sericite occurs as an alteration product of feldspar. Goethite forming after pyrite, orpheiite ($PbAl_3(PO_4,SO4)_2(OH)_6$), kaolinite and anatase are weathering products. Primary white mica is distinguished on the following textural criteria: it is euhedral, free of inclusions and not enclosed in any other mineral. Euhedral K-mica phenocrysts containing anatase crystals were possibly formed after magmatic biotite in the course of hydrothermal alteration. Based on microprobe analyses, both white mica phenocrysts and sericite are K-micas with moderate pyrophyllite and celadonite substitution. Their paragonite component (Na/Na+K) reaches 0.15 mol %. The similarity in chemical compositions of white K-mica phenocrysts and sericite, which are otherwise easy to distinguish from each other on textural grounds, is probably due to the fact that igneous muscovites re-equilibrated with hydrothermal fluids during alteration.

3.b. Orthogneiss

The orthogneisses within the metaclastic subunit (‘Kaesariani schists’) of the Basal Unit occur as lensoid to tabular bodies with intense deformation, especially at their margins. The dated sample was collected from a large outcrop close to Elaiochori village (east of Plaka, Fig. 2; coordinates: N 37°45′52″, E 24°0.3′33″). The presence of feldspar phenocrysts suggests that the precursor of this orthogneiss was a porphyritic igneous rock.

The common mineral assemblage is: white K-mica–plagioclase–K-feldspar–quartz–epidote–chlorite–apatite–titanite–calcite–Ti-oxides. Microprobe analyses of metamorphic white mica indicate that it is phengite with Si between 6.75 and 7.00 atoms p.f.u. Based on Massonne & Schreyer (1987), for an assumed T of 400–450 °C (Baziotis, Mposkos & Perdikatsis, 2006), these Si contents suggest pressures of ∼ 9–10.5 kbar and 12–13.5 kbar, respectively. The paragonite component reaches 0.05 mol %.

4. Analytical procedures and data evaluation

4.a. U–Pb SHRIMP dating

The age data were obtained on SHRIMP II at the Geological Survey of Canada, Ottawa. The spot size used for analysis was about 20 μm in diameter. For data collection, seven scans through the critical mass range were made. U/Pb ratios were calibrated relative to standard 6266, which is a piece of a Sri Lankan gem-quality zircon (see Stern & Amelin, 2003). Further details on the SHRIMP technique are to be found in Stern (1997) or Williams (1998).

4.b. Cathodoluminescence (CL) imaging

In order to investigate the existence of possibly different generations of zircon within the same crystal, CL and backscattered electron (BSE) images were obtained with a CamScan CS44LB, as well as a FEI Quanta 200 FEG instrument, at the Electron Microscopy Centre of ETH Zürich (EMEZ). CL images reveal the internal patterns of zircons, thus providing useful information on the formation history of the crystals and helping to avoid mixed ages of neighbouring zircon domains. In general, strong CL (bright appearance of the zircon) reflects low amounts of minor and trace elements, and weak CL (dark appearance of the zircon) reflects high amounts of minor and trace elements, including U (e.g. Sommerauer, 1974). Thus, the darker the zircon (weaker CL emission), the higher the U content. BSE and CL images were taken in sequence under the same instrumental conditions.

4.c. Data evaluation

The U–Pb SHRIMP data are presented in Table 1. For the calculation of the $^{206}Pb/^{238}U$ ratios and ages, the data were corrected for common Pb using the ^{207}Pb correction method following the standard procedures of Compston *et al.* (1992) and Williams, Buick & Cartwright (1996). The data are graphically presented on Tera-Wasserburg (TW) diagrams (Tera & Wasserburg, 1972), where total (uncorrected) $^{207}Pb/^{206}Pb$ versus the calibrated, total (uncorrected) $^{238}U/^{206}Pb$ ratio are plotted. The amount of common Pb was calculated using the isotope composition of surface common Pb at the Geological Survey of Canada (equal to a value of 0.895). In our samples, the amount of common

https://doi.org/10.1017/S0016756809006438 Published online by Cambridge University Press

Table 1. U, Th, Pb SHRIMP data for zircon from a granitoid sill and an orthogneiss of Lavrion area, SE Attica

Sample	U (ppm)	Th (ppm)	Th/U	rad. Pb	f_{206} %	$^{238}U/^{206}Pb$ (uncorrected)	(± 1σ)	$^{207}Pb/^{206}Pb$ (uncorrected)	(± 1σ)	Age±1σ (Ma) $^{206}Pb–^{238}U$
Granitoid sill										
Co-magmatic domains										
1. PAN1–9.1	1332	604	0.47	2	0.02	750.3	11.2	0.055	0.003	8.48 ± 0.13
2. PAN1–34.2	955	157	0.17	1	<0.01	766.7	12.8	0.055	0.009	8.29 ± 0.13
3. PAN1–31.1	1487	837	0.58	2	0.05	751.2	9.13	0.055	0.004	8.48 ± 0.13
4. PAN1–25.1	105	45	0.44	0	<0.01	676.0	35.2	0.135	0.041	8.54 ± 0.46
5. PAN1–26.1	298	98	0.34	0	<0.01	755.2	25.1	0.087	0.014	8.09 ± 0.25
6. PAN1–6.1	347	56	0.17	0	0.02	791.4	18.1	0.075	0.011	7.84 ± 0.19
7. PAN1–1.1	619	147	0.25	1	0.04	771.1	12.7	0.069	0.005	8.11 ± 0.13
										LI: 8.34 ± 0.20 Ma
Inherited granulite-type cores										
8. PAN1–9b.1	365	3.81	0.01	0	0.14	546.5	14.8	0.061	0.009	11.59 ± 0.32
9. PAN1–20.1	83	1.66	0.02	0	0.47	513.7	15.6	0.117	0.020	11.51 ± 0.35
10. PAN1–30.1	566	8.12	0.01	1	0.02	505.0	19.8	0.051	0.008	12.67 ± 0.51
11. PAN1–30b.1	64	0.63	0.01	0	0.47	458.3	12.8	0.157	0.018	12.20 ± 0.34
										LI: 11.93 ± 0.41 Ma
Orthogneiss										
Co-magmatic domains										
12. EL1–11.1	112	58	0.54	4	0.02	25.9	0.41	0.055	0.003	243 ± 4
13. EL1–2.1	322	351	1.12	15	<0.01	25.9	0.37	0.055	0.004	243 ± 4
14. EL1–6.1	174	139	0.83	7	0.07	25.5	0.32	0.090	0.004	236 ± 3
15. EL1–20.1	*85*	*52*	*0.63*	*3*	*0.02*	*27.5*	*0.37*	*0.055*	*0.003*	*229 ± 3*
16. EL1–7.1	*82*	*50*	*0.63*	*3*	*<0.01*	*27.6*	*0.47*	*0.059*	*0.004*	*228 ± 4*
										LI: 240 ± 4 Ma

Notes: LI: lower intercept; error on LI is given at the 95% confidence level; uncertainties are given at the 1σ level; f_{206} denotes the percentage of ^{206}Pb that is common Pb; analyses in italics (Nr. 15 and 16) were not considered for the LI calculation.

Pb was very low (analyses are plotted close to the concordia curve on the TW diagrams; see Section 5). The ellipses on the TW diagrams are plotted with a 2σ error. For the individual analyses listed in Table 1 and shown on the zircon CL images, 1σ errors are given. Finally, the ages were calculated from the lower intercept of the regression line with the concordia in the TW diagrams. The error on the lower intercept age is given at the 95 % confidence level (c.l.). For the diagrams and age calculations, the ISOPLOT program of Ludwig (2000) was used.

5. Zircon description and SHRIMP results

5.a. Granitoid sills

Zircons separated from the granitoid sill commonly occur as long-prismatic (~ 220–160 μm in length and ~ 100–80 μm in width) to equidimensional (~ 120 μm across) euhedral crystals. CL imaging revealed that most zircon crystals consist of two different domains: a round (resorbed) inner core with homogeneous CL surrounded by a rim with well-expressed oscillatory (magmatic) zoning (Fig. 4b and lower crystal of Fig. 4a). The resorbed character of the core, in combination with the homogeneous CL characteristics are features typically reported for zircons recrystallized under granulite-facies conditions (e.g. Vavra *et al.* 1996; Vavra, Schmid & Gebauer, 1999; Liati, Gebauer & Fanning, 2000). The presence of an inherited core in most zircon crystals strongly argues that the granitoid is of crustal origin. Some zircons of this rock are entirely oscillatory zoned (upper crystal of Fig. 4a).

Eleven spots were analysed on both zircon domains of this rock-type (Table 1): four are from the inherited zircon core domains and seven from the oscillatory zoned rims. On a Tera Wasserburg (TW) diagram (Fig. 5a), four analyses of the inherited cores define a mixing line between common Pb and a radiogenic $^{238}U/^{206}Pb$ end-member intersecting the concordia at 11.93 ± 0.41 Ma. The homogeneous CL, in combination with the low Th/U values of the core domains (0.01–0.02), are in line with a metamorphic origin of these domains (see, e.g. Hoskin & Schaltegger, 2003 and references therein). The oscillatory zoned euhedral rims surrounding the granulite-facies cores or occurring as single-domain crystals yielded a lower intercept age of 8.34 ± 0.20 Ma (Fig. 5b). This age is interpreted to reflect the time of magmatic crystallization of this igneous rock.

The homogeneous CL of the cores and their low Th/U ratios, compatible with a metamorphic origin, in combination with their round shape, commonly found in granulite-type metamorphic zircons, strongly suggest that metamorphism of the core domains of zircon reached granulite-facies conditions. As a result, complete recrystallization and resorption of the original zircon crystals took place (see Section 6).

5.b. Orthogneiss

Fifteen zircon crystals were recovered from the orthogneiss. They are relatively small (~ 100–160 μm in length and 60–80 μm in width), prismatic, euhedral crystals. In CL they exhibit a single domain with more or less expressed oscillatory zoning (Fig. 4c), indicative of magmatic origin.

https://doi.org/10.1017/S0016756809006438 Published online by Cambridge University Press

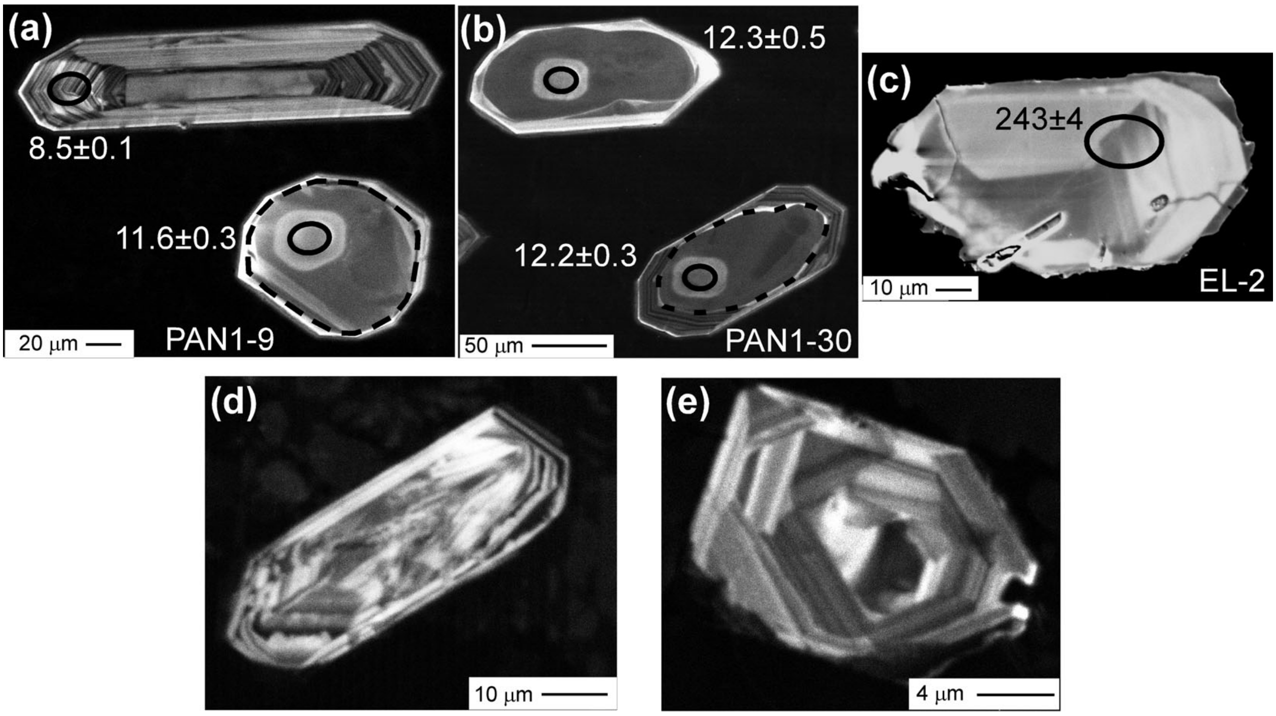

Figure 4. Cathodoluminescence (CL) images of selected zircon crystals from the granitoid sill (a, b) and the orthogneiss (c) of Lavrion area, SE Attica. CL images of two representative zircon crystals from a hornblende-bearing granitoid dyke (d) and from the granite of Plaka, Lavrion area (e) show that zircon in these rocks has no inherited cores. Dashed lines on the lower zircon crystals of (a) and (b) mark the limits between core and rim domains, for clarity. Note the round shape and homogeneous CL pattern in (b) and lower crystal of (a), indicative of granulite-facies metamorphism, as opposed to the oscillatory zoned (magmatic) CL pattern shown on upper crystal of (a) and on the rim of lower crystal in (b). Ellipses on the zircons correspond to SHRIMP spots. The bright area around the SHRIMP spots is due to rastering before SHRIMP analysis. Errors on the individual ages given on the CL images are 1σ. See also text for details.

Five spots were analysed from these zircons. On a TW diagram (Fig. 5c), three of them (analyses 12, 13 and 14 in Table 1) form a coherent grouping and plot on a mixing line with common Pb and a radiogenic $^{238}U/^{206}Pb$ as end-members and yield a lower intercept age of 240 ± 4 Ma. This age is interpreted as the time of crystallization of the magmatic protolith. The three analyses considered above for the lower intercept age calculation fit statistically on a single mixing line (dashed line in Fig. 5c) with the two analyses plotted as dashed ellipses in Figure 5c (analyses 15 and 16). This mixing line intersects the concordia at 236 ± 9 Ma, which is identical within error to the 240 ± 4 Ma age obtained above. However, the two youngest dates obtained by analyses 15 and 16 are probably reflecting partial Pb-loss caused by a post-crystallization metamorphic/fluid event. Therefore, we consider the oldest date (240 ± 4 Ma) as a more realistic approach for the age of the protolith.

6. Geodynamic implications

6.a. Granitoid sill

SHRIMP dating combined with CL-imaging of zircon from the granitoid sill revealed two different zircon generations with different CL and morphological characteristics recording the time of two different events, in which the present plutonic rock, as well as its precursor were involved: (1) a metamorphic event of the precursor rock at 11.93 ± 0.41 Ma, which probably reached granulite-facies conditions and resulted in the formation of round (resorbed) zircon cores with homogeneous CL and very low (metamorphic) Th/U ratios and (2) crystallization of the granitoid rock at 8.34 ± 0.20 Ma, which resulted in the formation of oscillatory zoned zircon precipitating from a melt. The 8.34 ± 0.20 Ma crystallization age of the granitoid sill is identical, within error, to the 8.27 ± 0.11 Ma K–Ar biotite age (Altherr *et al.* 1982) of the granitoid stock of Lavrion area and, statistically, marginally different from the 9.4 ± 0.3 Ma feldspar age reported for hornblende-bearing dykes below the detachment fault. These radiometric data indicate that igneous activity in the area took place either continuously between *c.* 8.3 and 9.4 Ma or that it evolved in different pulses within this time range.

Although a granulite-facies metamorphism is not proven with the present data nor recognized elsewhere in the Attic-Cycladic Belt on the basis of other criteria, it seems to be the most plausible hypothesis for the interpretation of the present data as: (1) it is consistent with the CL characteristics, low Th/U ratios and round morphology of the zircon cores and (2) the age of the cores is in line with the general extensional regime in the Aegean at that time. It is known that granulite-facies

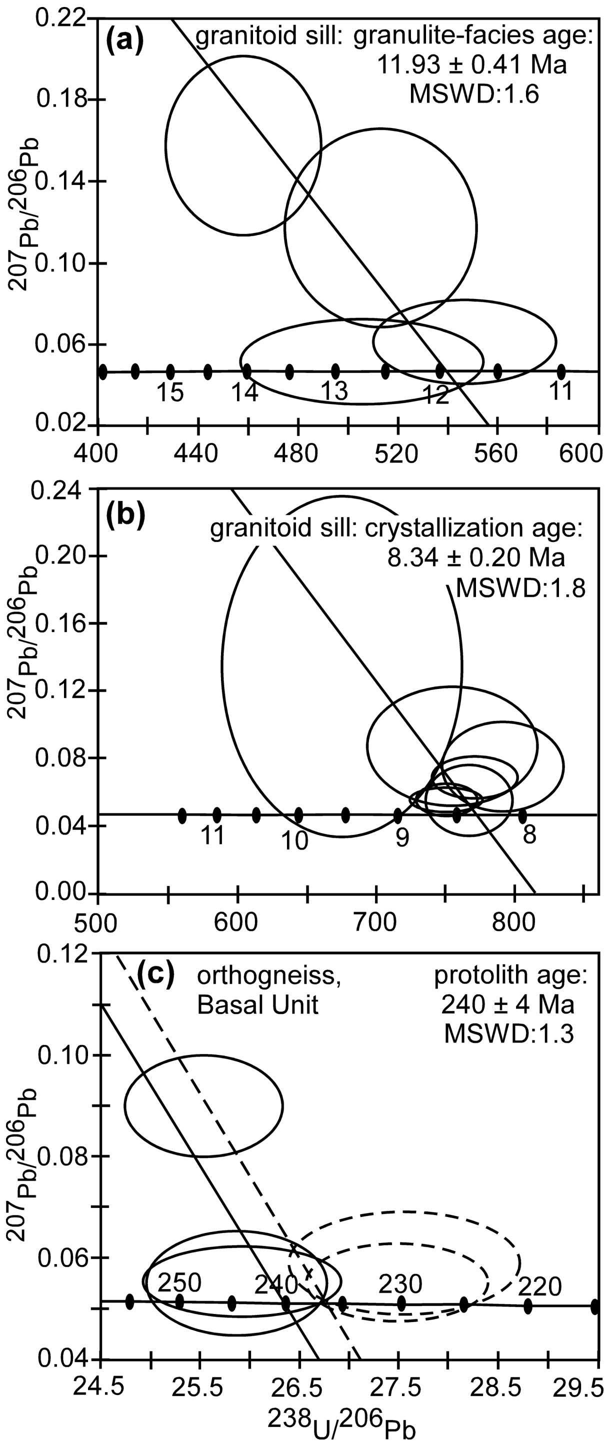

Figure 5. Tera-Wasserburg diagrams with data of zircons from the granitoid sill (a, b) and the orthogneiss (c) of Lavrion area. The ages are lower intercept ages and the errors are at the 95 % c.l. The ellipses are plotted with a 2σ error. The dashed line in (c) corresponds to the mixing line of all five analyses, including the ones yielding the youngest dates (dashed ellipses), which are probably due to partial Pb-loss. Consideration of the three oldest analyses for the lower intercept age calculation seems more plausible (see text for details).

metamorphism occurs as result of magmatic underplating of mafic magmas beneath continental areas at lower crustal levels, at the early stages of extension. Extension of continental crust started in the Aegean in Early Miocene times, accompanied by exhumation of HP rocks and amphibolite- to greenschist-facies metamorphism (e.g. Jolivet *et al*. 2003 and references therein). Most post-metamorphic igneous rocks in the Aegean are genetically connected to extensional tectonics and formation of core complexes and considered to have been derived from the sub-continental mantle (e.g. Pe-Piper & Piper, 2002 and references therein). Their formation precedes calc-alkaline volcanism in the Aegean arc, which started in Early Pliocene times. A likely granulite-facies metamorphism can be connected with magmatic underplating at 11.93 ± 0.41 Ma. The necessary heat input was probably high enough to cause granulite-facies metamorphism in rocks of the lower crust but did not lead to melting, as indicated by the absence of oscillatory zoned zircons of this age in the investigated rock. Partial melting, ascent and crystallization of the magma occurred later, at 8.34 ± 0.20 Ma (age of magmatic zircon), and produced the actual granitoid rocks in SE Attica. A likely mechanism for this partial melting, involving rapid ascent by pressure release, is in agreement with the fast operating detachment fault.

If the 11.93 ± 0.41 Ma age of the zircon cores indeed represents the time of granulite-facies metamorphism related to underplating and the initial stages of extension, this date sets an upper age limit for the operation of the detachment fault. The position of the granitoid sills on the hanging-wall of the detachment suggests that the detachment was still operating when these sills were emplaced at 8.34 ± 0.20 Ma. This interpretation implies that the time of the detachment activity in Lavrion is in line with the time of operation of detachment faults in the Cycladic islands. The main period of detachment faulting and magmatism in the Cyclades was *c*. 15–10 Ma, as suggested on the basis of low-temperature thermochronology (Brichau *et al.* 2006). Moreover, as suggested by Kumerics *et al.* (2005), most detachment faults in the Cyclades were active at least until 9 Ma, as in Naxos, Paros, Ios and Mykonos, or even later, as in Serifos and the East Aegean islands (Ikaria and Samos).

It is worth mentioning that CL imaging of numerous zircon crystals from both the hornblende-bearing granitoid dykes (I-type granitoids) in the footwall of the detachment fault and from the granodiorite stock of Plaka showed that they are devoid of inherited cores (Fig. 4d, e). Therefore, the dykes, which do not pierce the detachment, as well as the granitoid stock, are probably not fed by the same magma which formed the granitoid sills. It is noted that the zircons of the hornblende-bearing granitoid dykes and of the granodiorite stock of Plaka were not included for SHRIMP dating.

All magmatic rocks of the area were previously considered as apophyses of the late Miocene granodiorite of Lavrion (Marinos & Petrascheck, 1956) and therefore genetically connected to it. This interpretation is not supported by the new geochronological data obtained in this paper, nor by the variability in

https://doi.org/10.1017/S0016756809006438 Published online by Cambridge University Press

petrology and geochemistry of the stock, dykes and sills (Skarpelis, Tsikouras & Pe-Piper, 2008).

Carbonate-hosted replacement-type Pb–Ag–Zn massive sulphide ores, spatially associated to extensional structures in Lavrion and controlled by the detachment fault, are also temporally ascribed to the *c.* 12–8 Ma time span.

6.b. Orthogneiss

The SHRIMP age of 240 ± 4 Ma obtained for the protolith of the orthogneiss within the metaclastic subunit of the Basal Unit in SE Attica is comparable with both radiometric and biostratigraphic data on Early to Mid-Triassic metavolcanic and metatuffaceous rocks (*c.* 237–245 Ma) of the Cyclades (e.g. Pe-Piper & Piper, 2002; Tomaschek *et al.* 2003; Bröcker & Keasling, 2006; Bröcker & Pidgeon, 2007). Furthermore, Triassic to Jurassic fossils are reported from the Lower Marble of the Basal Unit in SE Attica (Marinos & Petrascheck, 1956), and the correlative Almyropotamos unit in Evia, which contains Late Triassic fossils (Katsikatsos, 1969). These rocks are the metamorphic equivalent to the Gavrovo-Tripolis Unit of the External Hellenide platform (Godfriaux, 1968), which comprises low-grade metaclastics with intercalated subalkaline volcanic rocks of Early to Mid-Triassic age (known as Tyros beds in Peloponnese and Crete) underlying neritic Mesozoic carbonate rocks. Triassic metavolcanic rocks and interbedded clastic sediments are also known from the Pelagonian terrane (Mountrakis *et al.* 1987; S. Keay, unpub. Ph.D. thesis, ANU, 1998; Pe-Piper & Piper, 2002; Anders, Reischmann & Kostopoulos, 2007).

7. Conclusions

(1) The SHRIMP results of the present paper, combined with previous radiometric data, indicate that late Miocene igneous activity in SE Attica took place between *c.* 8.3 and 9.4 Ma, either continuously or in different pulses (9.4 ± 0.3 Ma: age of hornblende-bearing dykes; 8.34 ± 0.20 Ma: age of the granitoid sills; 8.27 ± 0.11: age of the granodiorite stock).

(2) Contrary to earlier ideas about only Miocene magmatism in SE Attica, our data show that there is an age diversity of the meta-igneous protoliths (Early Triassic) and post-metamorphic igneous rocks (Late Miocene). The 240 ± 4 Ma Early Triassic protolith age of the orthogneiss dated here is consistent with the regional pattern of Triassic magmatism in the Hellenides.

(3) The granitoid sills contain zircons with granulite-type inherited cores, whereas I-type dykes and the granodiorite stock lack inherited cores, thus indicating different magma sources for the different igneous bodies. The source rock which provided the partial melts for the granitoid sills is probably not exposed on the surface.

(4) Metamorphism, probably reaching granulite-facies conditions, affected the precursor of the granitoid sills at 11.93 ± 0.41 Ma, as indicated by the CL and morphological characteristics of inherited zircon cores, as well as by their very low Th/U ratios. A likely granulite-facies metamorphism can be related to magmatic underplating at initial stages of extension, setting an upper age limit of 11.93 ± 0.41 Ma for the operation of the detachment fault.

(5) The age of granulite-facies metamorphism and that of subsequent magmatism, as obtained here from the granitoid sills, bracket the time span during which the Lavrion detachment fault was active between *c.* 11.9 and at least 8.3 Ma. This time span is in line with the time of detachment activity previously suggested for Cycladic islands.

(6) Deposition of carbonate-hosted replacement-type Pb–Ag–Zn massive sulphides, controlled by the detachment fault and associated extensional structures in the footwall, spatially associated to extensional structures in Lavrion and controlled by the detachment fault, is temporally ascribed also to the above time span of *c.* 12–8 Ma.

Acknowledgements. Thanks are due to N. Rayner and W. Davis, GSC Ottawa, for their valuable help during various stages of SHRIMP analytical work and data evaluation. The help of K. Kunze, EMEZ Center, ETH Zürich, during the SEM work for cathodoluminescence imaging is greatly appreciated. Many thanks also to Th. Theye, Stuttgart, for his help with the electron microprobe work and to D. Gebauer, ETH Zürich, for constructive discussions. Careful review and constructive suggestions by S. Brichau, University and Birkbeck College of London and D. Pyle, editor, Geological Magazine, are gratefully acknowledged. The work of AL was supported by a grant of the Swiss National Science Foundation (project No. 20–63767.00).

References

Altherr, R., Schliestedt, M., Okrusch, M., Seidel, E., Kreuzer, H., Harre, W., Lenz, H., Wendt, I. & Wagner, G. A. 1979. Geochronology of high-pressure rocks on Sifnos (Cyclades, Greece). *Contributions to Mineralogy and Petrology* **70**, 245–55.

Altherr, R., Kreuzer, H., Wendt, I., Lenz, H., Wagner, G. A., Keller, J., Harre, W. & Hohndorf, A. 1982. A Late Oligocene/Early Miocene high temperature belt in the Attic-Cycladic crystalline complex (SE Pelagonian, Greece). *Geologisches Jahrbuch* **E23**, 97–164.

Altherr, R. & Siebel, W. 2002. I-type plutonism in a continental back-arc setting: Miocene granitoids and monzonites from the central Aegean Sea, Greece. *Contributions to Mineralogy and Petrology* **143**, 397–415.

Anders, B., Reischmann, T. & Kostopoulos, D. 2007. Zircon geochronology of basement rocks from the Pelagonian Zone, Greece: constraints on the pre-Alpine evolution of the westernmost Internal Hellenides. *International Journal of Earth Sciences* **96**, 639–61.

Andriessen, P. A. M., Banga, G. & Hebeda, E. H. 1987. Isotopic age study of pre-Alpine rocks in the basal units on Naxos, Sikinos and Ios, Greek Cyclades. *Geologie en Mijnbouw* **66**, 3–14.

AVIGAD, D., GARFUNKEL, Z., JOLIVET, L. & AZANON, J. M. 1997. Back arc extension and denudation of Mediterranean eclogites. *Tectonics* **16**, 924–41.

BALTATZIS, E. 1996. Blueschist-to-greenschist transition and the P–T path of prasinites from the Lavrion area, Greece. *Mineralogical Magazine* **60**, 551–61.

BAZIOTIS, I., MPOSKOS, E. & PERDIKATSIS, V. 2006. Reconstruction and correlation of the exhumation history of high-pressure/low-temperature metamorphic rocks from Attica. *International Conference Neogene Magmatism of the Central Aegean and Adjacent Areas (NECAM): Petrology, Tectonics, Geodynamics, Mineral Resources and Environment*, Sept. 11–13, 2006, Milos, Cyclades, Greece. Book of Abstracts, p. 28.

BAZIOTIS, I., MPOSKOS, E. & SKARPELIS, N. 2006. Raman micro-spectrometry of carbonaceous material using the 633nm line of a He–Ne laser: application to the metamorphic rocks of Attica. *European Geosciences Union, Geophysical Research Abstracts* **8**, 10882.

BONNEAU, M. 1984. Correlation of the Hellenide nappes in the south-east Aegean and their tectonic reconstruction. In *Geological Evolution of the Eastern Mediterranean* (eds J. E. Dixon & A. H. F. Robertson), pp. 517–27. Geological Society of London, Special Publication no. 17.

BORONKAY, K. & DOUTSOS, T. 1994. Transpression and transtension within different structural levels in the central Aegean region. *Journal of Structural Geology* **16**, 1555–73.

BRICHAU, S., RING, U., KETCHAM, R. A., CARTER, A. STOCKLI, D. & BRUNEL, M. 2006. Constraining the long-term evolution of the slip rate for a major extensional fault system in the central Aegean, Greece, using thermochronology. *Earth and Planetary Science Letters* **24**, 293–306.

BRÖCKER, M. & KEASLING, A. 2006. Ionprobe U–Pb zircon ages from the high-pressure/low-temperature mėlange of Syros, Greece: age diversity and the importance of pre-Eocene subduction. *Journal of Metamorphic Geology* **24**, 615–31.

BRÖCKER, M. & PIDGEON, R. T. 2007. Protolith Ages of Meta-igneous and Metatuffaceous Rocks from the Cycladic Blueschist Unit, Greece: Results of a Reconnaissance U–Pb Zircon Study. *The Journal of Geology* **115**, 83–98.

BRÖCKER, M., KREUZER, H., MATTHEWS, A. & OKRUSCH, M. 1993. $^{39}Ar/^{40}Ar$ and oxygen isotope studies of polymetamorphism from Tinos island, Cycladic blueschist belt, Greece. *Journal of Metamorphic Geology* **11**, 223–40.

COMPSTON, W., WILLIAMS, I. S., KIRSCHVINK, J. L., ZICHAO, Z. & GUOGAN, M. 1992. Zircon U–Pb ages for the Early Cambrian time-scale. *Journal of the Geological Society, London* **149**, 171–84.

DÜRR, S., ALTHERR, R., KELLER, J., OKRUSCH, M. & SEIDEL, E. 1978. The median Aegean crystalline belt: stratigraphy, structure, metamorphism, magmatism. In *Alps, Apennines, Hellenides* (eds H. Cloos, D. Roeder & K. Schmidt), pp. 455–76. Stuttgart: Schweizerbart.

DUBOIS, R. & BIGNOT, G. 1979. Presence d'un "hard-ground" nummulitique au sommet de la serie cretacée d'Almyropotamos (Eubée méridionale, Grèce). Conséquences. *Comptes Rendus de l' Academie des Sciences de Paris* **289 D**, 993–5.

FAURE, M., BONNEAU, M. & PONS, J. 1991. Ductile deformation and syntectonic granite emplacement during the late Miocene extension of the Aegean (Greece). *Bulletin Société Géologique de France* **162**, 3–11.

FYTIKAS, M., INNOCENTI, F., MANETTI, P., MAZZUOLI, R., PECCERILLO, A. & VILLARI, L. 1984. Tertiary to Quaternary evolution of volcanism in the Aegean region. In *The geological evolution of the eastern Mediterranean* (eds A. H. F. Robertson & J. E. Dixon), pp. 687–99. Geological Society of London, Special Publication no. 17.

HENJES-KUNST, F. & KREUZER, H. 1982. Isotopic dating of pre-alpidic rocks from the island of Ios (Cyclades, Greece). *Contributions to Mineralogy and Petrology* **80**, 245–53.

HOSKIN, P. W. O. & SCHALTEGGER, U. 2003. The composition of zircon and igneous and metamorphic petrogenesis. In *Zircon* (eds M. J. Hanchar & P. W. O. Hoskin), pp. 27–62. *Reviews in Mineralogy and Geochemistry* **53**.

GODFRIAUX, I. 1968. Etude Géologique de la région de l'Olympe, Grèce. *Annales Géologiques des Pays Helléniques* **19**, 1–271.

JANSEN, J. B. H. & SCHUILING, R. D. 1976. Metamorphism on Naxos: Petrology and geothermal gradients. *American Journal of Science* **276**, 1225–53.

JOLIVET, L., FACCENNA, C., GOFFÉ, B., BUROV, E. & AGARD, F. 2003. Subduction tectonics and exhumation of high-pressure metamorphic rocks in the Mediterranean orogens. *American Journal of Science* **303**, 353–409.

KATSIKATSOS, G. 1969. Les formations triassiques de l'Eubée centrale. *Annales Géologiques des Pays Helléniques* **22**, 62–76.

KATSIKATSOS, G., MIGIROS, G., TRIANTAFYLLIS, M. & METTOS, A. 1986. Geological structure of Internal Hellenides (E. Thessaly – SW Macedonia, Euboea – Attica – Northern Cyclades Islands and Lesbos). *Geological and Geophysical Research, Special Issue*. I.G.M.E., Athens.

KEAY, S., LISTER, G. & BUICK, I. 2001. The timing of partial melting, Barrovian metamorphism and granite intrusion in the Naxos metamorphic core complex, Cyclades, Aegean Sea, Greece. *Tectonophysics* **342**, 275–312.

KUMERICS, C., RING, U., BRICHAU, S., GLODNY, J. & MONIÉ, P. 2005. The extensional Messaria shear zone and associated brittle detachment faults, Aegean Sea, Greece. *Journal of the Geological Society* **162**, 701–21.

LIATI, A., GEBAUER, D. & FANNING, M. C. 2000. U–Pb SHRIMP dating of zircon from the Novate granite (Bergell, Central Alps): evidence for Oligocene–Miocene magmatism, Jurassic–Cretaceous continental rifting and opening of the Valais trough. *Schweizerische Mineralogische Petrographische Mitteilungen* **80**, 305–16.

LEE, J. & LISTER, G. S. 1992. Late Miocene ductile extension and detachment faulting, Mykonos, Greece. *Geology* **20**, 121–4.

LELEU, M. & NEUMANN, M. 1969. L'âge des formations d'Attique: du paleozoique au mesozoique. *Comptes Rendu de l'Academie des Sciences de Paris* **268**, 1361–3.

LISTER, G. S., BANGA, G. & FEENSTRA, A. 1984. Metamorphic core complexes of the Cordilleran type in the Cyclades, Aegean Sea, Greece. *Geology* **12**, 221–5.

LUDWIG, K. 2000. *User's Manual for Isoplot/Ex, version 2.4. A geochronological Toolkit for Microsoft Excel*. Berkeley Geochronological Center, Special Publication no. 1a, 53 pp.

MARINOS, G. P. & PETRASCHECK, W. E. 1956. Laurium. *Geological & Geophysical Research* **4/1,** pp. 1–247. Institute for Geology and Subsurface Research.

MASSONNE, H. J. & SCHREYER, W. 1987. Phengite geobarometry based on the limiting assemblage with K-feldspar,

phlogopite and quartz. *Contributions to Mineralogy and Petrology* **96**, 212–24.
MATTHEWS, A. & SCHLIESTEDT, M. 1984. Evolution of the blueschist and greenschist facies rocks of Sifnos, Cyclades, Greece.*Contributions to Mineralogy and Petrology* **88**, 150–63.
MCKENZIE, D. 1978. Active tectonics of the Alpine–Himalayan belt: The Aegean Sea and surrounding regions. *Royal Astronomical Society Geophysical Journal* **55**, 217–54.
MOUNTRAKIS, D., ELEFTHERIADIS, G., CHRISTOFIDES, G., KILIAS, A. & SAPOUNTZIS, E. 1987. Silicic Metavolcanics in the Western Pelagonian Margin of Greece Related to the Opening of Neo-Tethys. *Chemie der Erde* **47**, 167–79.
OKRUSCH, M. & BRÖCKER, M. 1990. Eclogite facies rocks in the Cycladic blueschist belt, Greece: A review. *European Journal of Mineralogy* **2**, 451–78.
PE-PIPER, G. 2000. Origin of S-type granites coeval with I-type granites in the Hellenic subduction system, Miocene of Naxos, Greece. *European Journal of Mineralogy* **12**, 859–75.
PE-PIPER, G. & PIPER, D. J. W. 2002. *The igneous rocks of Greece: anatomy of an orogen. Beitrage zur Regionalen Geologie der Erde*. Berlin, Stuttgart: Gebrüder Borntrager, 573 pp.
PE-PIPER, G., KOTOPOULI, C. N. & PIPER, D. J. W. 1997. Granitoid rocks of Naxos, Greece: regional geology and petrology. *Geological Journal* **32**, 153–71.
PE-PIPER, G., PIPER, D. J. W. & MATARANGAS, D. 2002. Regional implications of geochemistry and style of emplacement of Miocene I-type diorite and granite, Delos, Cyclades, Greece. *Lithos* **60**, 47–66.
RING, U. & REISCHMANN, T. 2002. The weak and superfast Cretan detachment, Greece: exhumation at subduction rates in extruding wedges. *Journal of the Geological Society, London* **159**, 225–8.
RING, U., LAYER, P. W. & REISCHMANN, T. 2001. Miocene high-pressure metamorphism in the Cyclades and Crete, Aegean Sea, Greece: Evidence for large-scale magnitude displacement on the Cretan detachment. *Geology* **29**, 395–8.
SHAKED, Y., AVIGAD, D. & GARFUNKEL, Z. 2000. Alpine high-pressure metamorphism at the Almyropotamos window (southern Evia, Greece). *Geological Magazine* **137**, 367–80.
SKARPELIS, N. & GILG, A. H. 2006. Miocene extensional fault-controlled mineralization in the central Aegean (Mykonos, Cyclades): deposition from a two-stage hydrothermal system? *International Conference Neogene Magmatism of the Central Aegean and Adjacent Areas (NECAM): Petrology, Tectonics, Geodynamics, Mineral Resources and Environment.* Sept. 11–13, 2006, Milos, Cyclades, Greece, p. 36.
SKARPELIS, N. 2007. The Lavrion deposit: geology, mineralogy and minor elements chemistry. *Neues Jahrbuch Mineralogie, Abhandlungen* **183/3**, 722–94.
SKARPELIS, N., TSIKOURAS, B. & PE-PIPER, G. 2008. The Miocene igneous rocks in the Basal Unit of Lavrion (SE Attica, Greece): petrology and geodynamic implications. *Geological Magazine* **145**, 1–15.
SOMMERAUER, J. 1974. Trace elements distribution patterns and mineralogical stability of zircons – An application for combined electron microprobe techniques. *Electron Microscopy Society of Southern Africa, Proceedings* **4**, 71–2.
STERN, R. 1997. The GSC Sensitive High Resolution Ion Microprobe (SHRIMP): analytical techniques of zircon U–Th–Pb age determinations and performance evaluation. *Radiogenic Age and isotope studies: Report 10. Geological Survey of Canada, Current Research*, 1–31.
STERN, R. A. & AMELIN, Y. 2003. Assessment of errors in SIMS zircon U–Pb geochronology using a natural zircon standard and NIST SRM 610 glass. *Chemical Geology* **197**, 1–32.
TERA, F. & WASSERBURG, G. J. 1972. U–Th–Pb systematics in three Apollo 14 basalts and the problem of initial Pb in lunar rocks. *Earth and Planetary Science Letters* **14**, 281–304.
TOMASCHEK, F., KENNEDY, A. K., VILLA, I. M., LAGOS, M. & BALLHAUS, C. 2003. Zircons from Syros, Cyclades, Greece – Recrystallization and mobilization of zircon during high-pressure metamorphism. *Journal of Petrology* **44**, 1977–2002.
VAVRA, G., GEBAUER, D., SCHMID, R. & COMPSTON, W. 1996. Multiple zircon growth and recrystallization during polyphase Late Carboniferous to Triassic metamorphism in granulites of the Ivrea Zone (Southern Alps): an ion microprobe (SHRIMP) study. *Contributions to Mineralogy and Petrology* **122**, 337–58.
VAVRA, G., SCHMID, R. & GEBAUER, D. 1999. Internal morphology, habit and U–Th–Pb microanalysis of amphibolite-to-granulite facies zircons: geochronology of the Ivrea Zone (Southern Alps). *Contributions to Mineralogy and Petrology* **134**, 380–404.
WIJBRANS, J. R. & MCDOUGALL, I. 1988. Metamorphic evolution of the Attic-Cycladic Metamorphic Belt on Naxos (Cyclades, Greece) utilizing $^{40}Ar/^{39}Ar$ age spectrum measurements. *Journal of Metamorphic Geology* **6**, 571–94.
WILLIAMS, I. S. 1998. U–Th–Pb Geochronology by Ion Microprobe. In *Applications of microanalytical techniques to understanding mineralizing processes* (eds M. A. McKibben, W. C. Shanks, III & W. I. Ridley), pp. 1–35. *Reviews in Economic Geology* **7**.
WILLIAMS, I. S., BUICK, S. & CARTWRIGHT, I. 1996. An extended episode of early Mesoproterozoic metamorphic fluid flow in the Reynolds Range, central Australia. *Journal of Metamorphic Geology* **14**, 29–47.